AGU PUBLICATIONS

JGR

Journal of Geophysical Research: Atmospheres

RESEARCH ARTICLE
10.1002/2015JD023646

Key Points:
- Volatility measurements of monodisperse nanoparticles in the high Arctic
- Compounds involved in particle growth during nucleation are indirectly identified
- Findings show that 12 nm particles mainly consist of ammoniated sulfates

Correspondence to:
K. Eleftheriadis,
eleftheriadis@ipta.demokritos.gr

Citation:
Giamarelou, M., K. Eleftheriadis, S. Nyeki, P. Tunved, K. Torseth, and G. Biskos (2016), Indirect evidence of the composition of nucleation mode atmospheric particles in the high Arctic, *J. Geophys. Res. Atmos.*, *121*, 965–975, doi:10.1002/2015JD023646.

Received 8 MAY 2015
Accepted 5 JAN 2016
Accepted article online 10 JAN 2016
Published online 30 JAN 2016

Indirect evidence of the composition of nucleation mode atmospheric particles in the high Arctic

Maria Giamarelou[1], Konstantinos Eleftheriadis[2], Stephan Nyeki[3], Peter Tunved[4,5], Kjetil Torseth[6], and George Biskos[7,8]

[1]Department of Environment, University of the Aegean, Mytilene, Greece, [2]Environmental Radioactivity Laboratory, INRaSTES, NCSR Demokritos, Athens, Greece, [3]Physical-Meteorological Observatory, World Radiation Center, Davos, Switzerland, [4]Department of Applied Environmental Science, Stockholm University, Stockholm, Sweden, [5]Bert Bolin Centre for Climate Research, Stockholm University, Stockholm, Sweden, [6]Norwegian Institute For Air Research, Kjeller, Norway, [7]Faculty of Civil Engineering and Geoscience, Delft University of Technology, Delft, Netherlands, [8]Energy Environment and Water Research Center, The Cyprus Institute, Nicosia, Cyprus

Abstract Previous long-term observations have shown that nanoparticle formation events are common in the summer-time high Arctic and linked to local photochemical activity. However, current knowledge is limited with respect to the chemical precursors of resulting nanoparticles and the compounds involved in their subsequent growth. Here we report case-study measurements during new particle formation (NPF) events of the particle size distribution (diameter > 7 nm) and for the first time the volatility of monodisperse particles having diameter $\leq$40 nm, providing indirect information about their composition. Volatility measurements provide indirect evidence that a predominant fraction of the 12 nm particle population is ammoniated sulfates in the summertime high Arctic. Our observations further suggest that the majority of the sub-40 nm particle population during NPF events does not exist in the form of sulfuric acid but rather as partly or fully neutralized ammoniated sulfates.

1. Introduction

Quantifying the effect of natural and anthropogenic particles on regional and global climate requires information of their size and chemical composition. Although new particle formation (NPF) events have been observed in many locations around the globe [*Kulmala et al*., 2004] and are common in the high Arctic during summer [*Leck and Bigg*, 2010; *Karl et al*., 2012; *Leaitch et al*., 2013; *Tunved et al*., 2013], the mechanisms leading to such events are only beginning to be fully understood [*Kuang et al*., 2010; *Karl et al*., 2013; *Kulmala et al*., 2013]. Sulfuric acid, formed by the oxidation of sulfur dioxide (originating either from anthropogenic emissions or from oxidation of marine dimethyl sulfide [*Chang et al*., 2011]) in the presence of water vapor, is suggested to be involved in NPF and growth of atmospheric particles [*Weber et al*., 1996; *Sipila et al*., 2010]. However, other components such as ammonia [*Korhonen et al*., 1999], marine iodine compounds [*O'Dowd et al*., 2002], amines [*Smith et al*., 2010; *Paasonen et al*., 2012], condensable organic constituents [*Riipinen et al*., 2012; *Ehn et al*., 2014], and nanogel fragments (i.e., building blocks of airborne marine gels that form after evaporation of fog and clouds) [*Leck and Bigg*, 1999, 2005, 2010; *Karl et al*., 2013] are also considered to participate to varying degrees in NPF events and growth.

Earlier studies, based on chemical composition [*Heintzenberg and Leck*, 1994] and particle size distribution [*Covert and Heintzenberg*, 1993; *Wiedensohler et al*., 1996; *Nyeki et al*., 2005] measurements, have suggested that NPF events in the high Arctic are mainly caused by photochemical activity involving the gas-phase formation of sulfuric acid. All chemical composition measurements to date, however, have used filter and impactor samples collected over hours to days. As a result, their association with nanoparticle formation and growth events has not been possible. Several microscope studies have also been conducted on particles in the Arctic. *Bigg and Leck* [2001] observed that particle growth up to $D_p \sim 50$ nm did not appear to be controlled by sulfuric acid or other DMS oxidation products in the high Arctic. On the other hand, larger particles were associated with these compounds. *Geng et al*. [2010] conducted single-particle analysis on atmospheric particles on Svalbard and observed that sulfates and nitrates were present in the particle phase. However, these observations are not directly linked to NPF events.

Measuring the chemical composition of nanoparticles at a high temporal resolution in background/remote regions is a challenge even for state-of-the-art aerosol mass spectrometers due to their low mass concentrations and small sizes. Alternatively, a way of indirectly probing nanoparticle chemical composition is by measuring their integral properties such as volatility and/or hygroscopicity [*Sakurai et al*., 2005; *Frey et al*., 2008], both of which offer relatively robust constraints on their composition. Previous volatility studies in the high Arctic have either concerned the observation of large monodisperse ($D_p \sim 200$ nm) [*Covert and Heintzenberg*, 1993] or polydisperse [*Eleftheriadis et al*., 2004; *Nyeki et al*., 2005] particles. However, the latter method cannot be used to indirectly determine their size-resolved composition.

In this study, we characterize atmospheric aerosols observed in the summertime high Arctic using high temporal resolution (15–20 min) measurements of (1) the particle size distribution by a Differential Mobility Particles Sizer (DMPS) and (2) the volatility of monodisperse particles by a Volatility Tandem Differential Mobility Analyzer (VTDMA) system.

2. Materials and Methods

Measurements took place at the Zeppelin atmospheric research station (78.90°N, 11.88°E; 474 m above sea level (asl)) near Ny-Ålesund, Svalbard, from 15 June to 6 July 2008 (day of year; DOY 167–187). Atmospheric aerosol particles were sampled through an all-weather roof-top inlet on Zeppelin station. By using a high flow rate of 35 lpm, from which instruments subsampled, losses in the main inlet were minimized. Components of the main and subsampling tubes were stainless-steel, resulting in a sample temperature of ~21°C (<20% RH) before reaching the instruments. Considering that all the instruments used the same sampling tubes, all measured particles would be free of any possible compounds that would volatilize at room temperature.

An ultrafine Condensation Particle Counter (CPC), a DMPS [*Keady et al*., 1983], and a Volatility Tandem Differential Mobility Analyzer (VTDMA) were used to measure the total number concentration (N), the number size distribution, and the volatility of atmospheric particles, respectively. The CPC (TSI Model 3025) had a theoretical cutoff detection limit at $D_p = 3$ nm [*Stolzenburg and McMurry*, 1991] and was operated with a 1.5 lpm flow rate. In addition, the sampling time was increased to 3 min in order to improve the counting statistics to within less than 10% [*McMurry*, 2000]. The DMPS consisted of a medium-sized Hauke-type Differential Mobility Analyzer (DMA) and another CPC (TSI Model 3760). A neutralizer was used to establish an equilibrium charge distribution on the particles before entering the DMA where they were classified according to their electrical mobility. The aerosol and sheath flow rates through the DMA were adjusted to 1.5 and 10 lpm, respectively, during the entire case study. With these settings, the system was capable of measuring the particle size distribution in the $D_p = 10$–635 nm range every 20 min. Particle number concentrations in the $D_p = 3$–10 nm range (N_{3-10}) were obtained by subtracting DMPS from CPC data.

The VTDMA [*Mendes et al*., 2016] consisted of a ^{85}Kr aerosol neutralizer, two custom-made DMAs, a temperature-controlled thermodenuder placed between both DMAs, and a CPC (TSI Model 3025) downstream of the second DMA. The sampled polydisperse particles were passed through the ^{85}Kr aerosol neutralizer and the first DMA, in which the applied voltage between both electrodes was adjusted to select monodisperse particles with $D_p = 12$, 40, 150, and 200 nm. Particles then passed through an improved low-flow thermodenuder [*Fierz et al*., 2007] and were exposed to temperatures T_D of 30, 120, and 230°C in the heating section (10 cm long), followed by gradual cooling in the absorption section (20 cm long), before their size distribution from $D_p = 7$ to 280 nm was measured with the second DMA and the CPC. The aerosol residence time in the thermodenuder and absorption section was 1.0 s. This improved design allowed more flexibility in setting the temperature profile along the thermodenuder and allowed retention of gas-phase volatile compounds in the absorption section without re-condensation [*Mendes et al*., 2016]. Both DMAs employed a closed-loop recirculation system for the sheath flow, which was adjusted to 5.5 lpm, while the aerosol flow rate was 1.5 lpm through the VTDMA. Each VTDMA measurement cycle at a specific thermodenuder temperature and monodisperse particle size took 15 min in order to ensure adequate counting statistics.

Depending on their composition, monodisperse particles will behave differently in a thermodenuder. For instance, sulfuric acid particles will evaporate completely at $T_D \geq 120$°C and ammoniated sulfates at $T_D \geq 230$°C [*Clarke*, 1991]. Refractory particles such as NaCl, black carbon (BC) or marine polymer gels will not change in size nor will their concentration decrease when exposed to these temperatures. Such behavior

is in contrast to organic compounds, which typically consist of a complex rather than a simple mixture of organic compounds [*Tunved et al*., 2006; *Riipinen et al*., 2012; *Zhang et al*., 2012]. As a consequence, organic particles exhibit a smooth rather than a "stepwise " temperature dependence in thermodenuders due to their different volatility characteristics [*Hakkinen et al*., 2012]. The ability to characterize a mixture of organic compounds in a thermodenuder is thus rather limited. To fully characterize the performance of the VTDMA at different T_D, the system was characterized with nonorganic and organic coated laboratory-generated particles before field deployment [*Mendes et al*., 2016]. First, particle losses in the VTDMA were determined to be $<$15% for $D_p = 10$ nm, and $<$5% for Aitken/Accumulation mode particles at all T_D, during calibration with monodisperse NaCl particles. All data were corrected for these losses. Second, the efficiency of the system to completely evaporate ammonium sulfate particles at $T_D = 230$°C (1.5 lpm aerosol flow-rate, 1.0 s residence time) was confirmed as in other studies [*Villani et al*., 2007]. Polydisperse ammonium sulfate particles were generated by atomizing a 1% aqueous solution in an atomizer particle generator (TOPAS Model ATM220), and dried to $<$20% RH in a diffusion drier. The behavior of ammonium sulfate particles was then characterized in the VTDMA, by conducting a temperature scan up to 250°C at 10°C steps. A reduction in N was not observed at $T_D = 30$ or 120°C. However, N began to reduce at ~200°C and had reduced by 95–98% at 230°C for particles over the measurable size range down to $D_p \sim 18$–20 nm [*Mendes et al*., 2016]. These properties of a thermodenuder offer a relatively robust constraint on the presence of pure sulfuric acid and ammoniated sulfates in atmospheric particles.

Zeppelin station belongs to the "Co-operative Programme for Monitoring and Evaluation of the Long-range Transmission of Air Pollutants in Europe" (EMEP). Daily measurements of SO_2 and NH_3 have been conducted since 1989 [*Aas et al*., 2012]. The major objective is to monitor long-term spatial and temporal trends in a network of about 100 sites across Europe, and the methodology was selected to allow the determination of ambient levels throughout the network in a cost-efficient and comparable way [*Tørseth et al*., 2012]. The method employed is based on sampling with a filter-pack consisting of a first-stage particle filter, followed by a second-stage potassium hydroxide impregnated filter for SO_2 absorption and a third-stage oxalic acid impregnated filter for NH_3 absorption, and off-line determination by ion chromatography. The method and its uncertainties is described in an EMEP publication [*Co-operative Programme for Monitoring and Evaluation of the Long-range Transmission of Air Pollutants in Europe (EMEP)*, 2014], and the Norwegian Institute for Air Research (NILU) has accreditation for the method according to NS-EN ISO/IEC 17025. It should be noted, however, that while the SO_2 detection limit is low (~0.01 μg S m^{-3} = 4 parts per trillion by volume (pptv)), that for NH_3 measurements is higher (~0.05 μg N m^{-3} = 72 pptv) due to problems with filter contamination and the fact that the filter-pack method is biased when it comes to separating gaseous and particulate nitrogen species. As ambient levels of SO_2 and NH_3 at Zeppelin during the experiment were very low, and close to the levels of detection, interpretation of the filter pack results must be treated with care. Although data from 24 h filter-pack sampling present a limitation in comparison with data of better time resolution, it allows a low detection limit to be attained. Despite these limitations, we have chosen to include the data due to its availability from the ongoing monitoring program. Although only daily average concentrations were available from NILU, they do at least allow an estimate of H_2SO_4 concentrations ($[H_2SO_4]$) to be made when the global irradiation and relative humidity are used as inputs to a model. Values of $[H_2SO_4]$ may then help to interpret VTDMA results.

BC concentration was measured using an Aethalometer (Magee Scientific Model AE-31) with a 30 min time resolution. UV and global irradiation measurements were conducted with a Total Ultraviolet Radiometer (Eppley Laboratory, Inc.; $\lambda = 295$–385 nm), and a Pyranometer (Kipp and Zonen Model CMP22; $\lambda = 0.3$–2.8 μm), respectively.

Evidence for long-range transport of clean or polluted air masses was obtained from 5 day back trajectory analysis using the NOAA Hybrid Single-Particle Lagrangian Integrated Trajectory (HYSPLIT) model [*Draxler and Hess*, 1997; *Draxler and Rolph*, 2015]. Two and 5 day back-trajectories were investigated for three different arrival heights (station altitude i.e., 474 m, as well as 1000 and 1500 m). As the results were similar in all cases, 5 day back-trajectories for Zeppelin station height arriving at 12:00 UTC were considered further. Limitations in using back-trajectories are discussed elsewhere [*Draxler and Hess*, 1997; *Draxler and Rolph*, 2015] but it should be noted that uncertainties in determining source regions will exist as re-analysis data used by HYPSLIT is based on a sparse network of meteorological measurements in the Arctic. In addition, the effect of the boundary layer is not considered in this version of the model.

3. Results and Discussion

The identification of extended and substantial new particle growth events was based on the criterion that $N_{3-10} > N_{10-635}$ (particle diameter range given in subscript) by at least 10% for ~6 h. In this manner, five events lasting from ~10 to 13 h were identified and are indicated in Figures 1, and 3 by the shaded areas. A sixth event was also identified when particle volatility but not size distribution measurements were available. NPF events in Figure 1a are reflected in elevated values of N_{3-10} and N_{10-30}, with averages ~600 and 4100 cm^{-3}, respectively, as opposed to ~150 and 1300 cm^{-3} during all other periods. It should also be pointed out that the nucleation dynamics can vary between the events, leading to small lags in the evolution of N_{3-10} and N_{10-30} in some cases.

The UV irradiation exhibited a diurnal pattern with maximum values on event days that varied from 18 to 32 W m^{-2}. The ambient temperature varied from −2 to 8°C during the entire case study, and from 0 to 7°C during NPF events. RH generally varied from 60 to 90% during NPF events except for a brief decrease to ~40% on DOY 180. All events occurred under clear skies or moderate/low (<25%) cloud coverage as indicated by short-wave downward irradiation (not shown). Despite the continuous daylight during the case-study, new particles in the range D_p = 3–10 nm (Figure 1b) were first observed around midday by our instruments when UV irradiation exhibited maximum values >25 W m^{-2} (Figure 1c).

Daily precursor gas measurements of SO_2 and NH_3 (Figure 1d) gave average concentrations ~0.03 μg S m^{-3} (11 pptv) and 0.18 μg N m^{-3} (257 pptv), which are comparable to long-term averages of ~0.07 μg S m^{-3} (26 pptv) [*Engvall et al.*, 2008] and 0.17 μg N m^{-3} (243 pptv), respectively. To identify NPF events attributable to local anthropogenic pollution, Figure 1d also shows the aerosol BC concentration whose average value of ~10 ng m^{-3} is typical of summer periods (5–15 ng m^{-3}) from long-term measurements [*Eleftheriadis et al.*, 2009]. Two local ship pollution episodes occurred on DOY 178 and 181, as indicated by the sharp spikes in BC concentration. Interestingly, NPF events were not observed during these episodes or thereafter, indicating that emitted gases did not directly result in NPF. Air masses arriving at Zeppelin station during events were found to originate from the high Arctic (latitudes >70°N, see Figure 2) and had been confined to a layer <1000 m asl along their paths. In addition, air masses had spent >95% time over sea pack-ice or snow/ice-covered land, suggesting that they were representative of background Arctic conditions (the sea ice concentration corresponded to the average June 2008 coverage [*National Snow & and Ice Data Center (NSIDC)*, 2014]. However, evidence of a long-range pollution episode on DOY 173–175 is visible as a weak peak in BC concentration. Five-day back trajectory analysis indicated an origin over the central Arctic and north of Greenland, which has been previously identified as a region where NPF events occur [*Leaitch et al.*, 2013]. VTDMA results discussed further below (Figure 4), however suggest that the NPF event on DOY 173 occurred in an air mass influenced by long-range transported anthropogenic pollution. Based on these observations, four NPF events (light shaded periods; Figure 1d) were deemed to have occurred in background Arctic air masses, while the other two (dark shaded) were deemed to have an anthropogenic influence. The four events can be described as "regional" where NPF events and growth occur fairly uniformly over several hours to days throughout the air mass [*Kulmala et al.*, 2004]. It should be noted that the use of back trajectory analysis is only used here to select NPF events, which are most probably associated with background Arctic air masses. We are not able to gain any insight into meteorological conditions over the sea ice interface.

Returning to the NPF events in Figure 1a, it was determined that the average growth rates of recently nucleated particles were ≤1.0 nm h^{-1} for the range D_p = 10–20 nm. Similarly, low values for the same range have been previously observed in sub-Arctic and Antarctic regions [*Kulmala et al.*, 2004; *Engvall et al.*, 2008; *Zhang et al.*, 2012, and references therein]. Current models [*Yli-Juuti et al.*, 2013] and observations [*Yli-Juuti et al.*, 2011] suggest that sulfuric acid together with organic compounds (acids, terpenes, and amines) can contribute to the growth of nanoparticles with D_p = 3–20 nm, which can yield growth rates of up to 3.0 nm h^{-1} even in remote environments with low precursor concentrations. In the absence of organic compounds, however, observed growth rates are limited [*Yli-Juuti et al.*, 2011] and are comparable to our observations, which indirectly implies that sulfuric acid may be the dominant precursor for nanoparticle growth in the region. Amines in particular can enhance nucleation rates at low H_2SO_4 concentrations by forming stable acid–base pairs [*Chen et al.*, 2012; *Almeida et al.*, 2013;

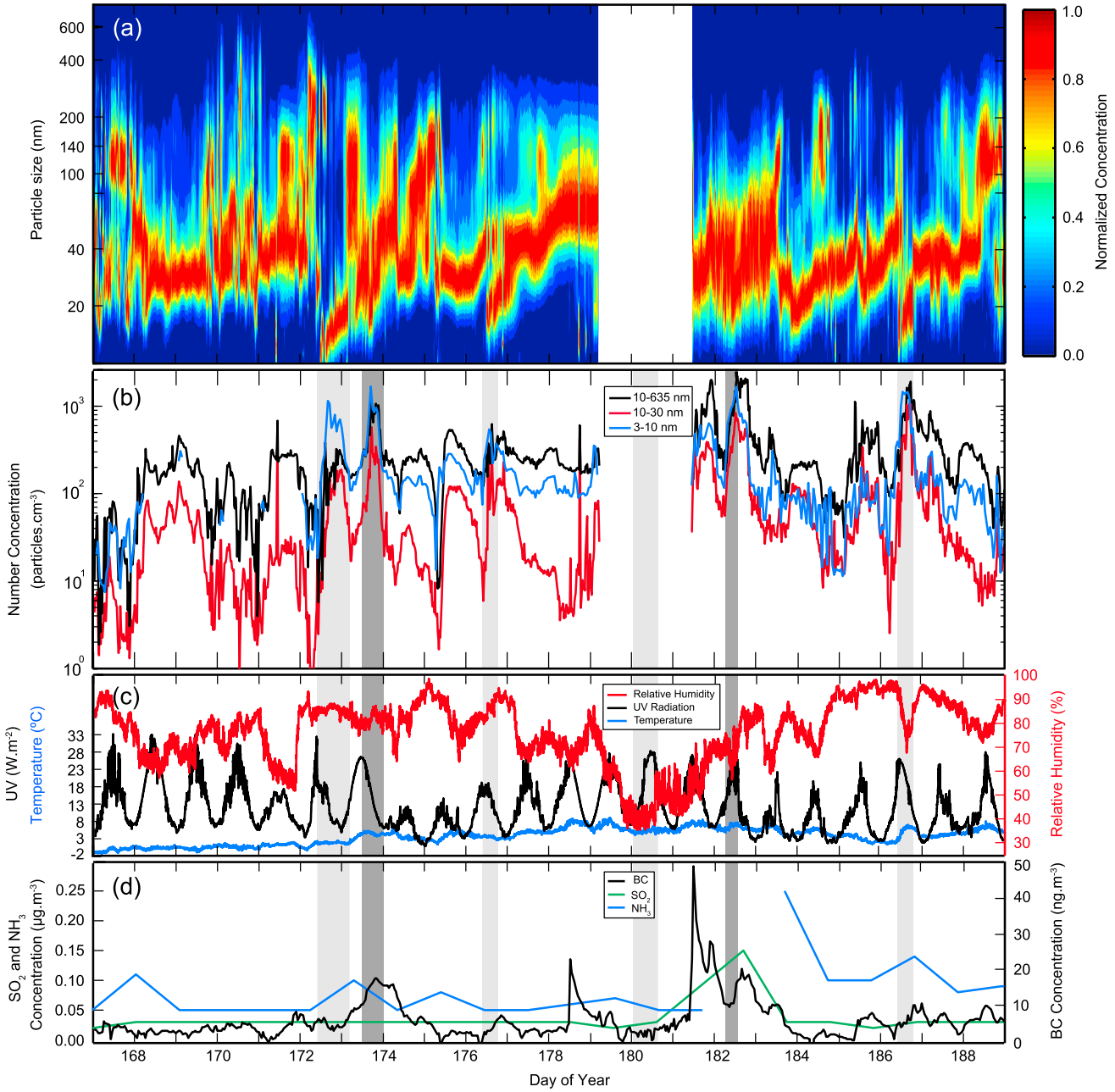

Figure 1. Evolution of particle size distributions, meteorological parameters, and concentrations of gaseous compounds measured at Ny-Ålesund from 15 June (DOY 167) to 7 July (DOY 189) 2008. (a) Normalized particle number size distributions. (b) Hourly average particle number concentrations for the size ranges: D_p = 10–635 nm (black line), D_p = 10–30 nm (red line), and D_p = 3–10 nm (blue line). (c) Hourly average ambient temperature (blue line), UV irradiation (black line), and relative humidity RH (red line). (d) Concentrations of BC, SO_2, and NH_3 (black, red, and blue lines, respectively). NPF events occurring on 20–21, 21, 24, and 30 June (DOY 172–173, 173, 176, and 182) and 4 July (DOY 186) are indicated by the light shaded (background Arctic air masses) and dark shaded (anthropogenically influenced) periods, which had an average duration of 13.4 and 10.4 h, respectively. Identification of the event on 28 June (DOY 180) was based on VTDMA results (cf. Figure 4).

Riccobono et al., 2014]. For instance, alkylamines have been found to readily react with sulfuric acid to give alkylaminium sulfate [*Wang et al.*, 2010]. While amines and NH_3 have similar sources over land (e.g., agricultural activity, biomass burning, soils and vegetation) and ocean (e.g., bacterial decomposition of organic matter and phytoplankton excretion) regions, concentrations of the former are generally $\lesssim$20% of the latter in low to midlatitude regions [*Ge et al.*, 2010]. Very few measurements have been conducted in the sub-Arctic let alone the high Arctic. A study in a sub-Arctic boreal forest using a thermal desorption

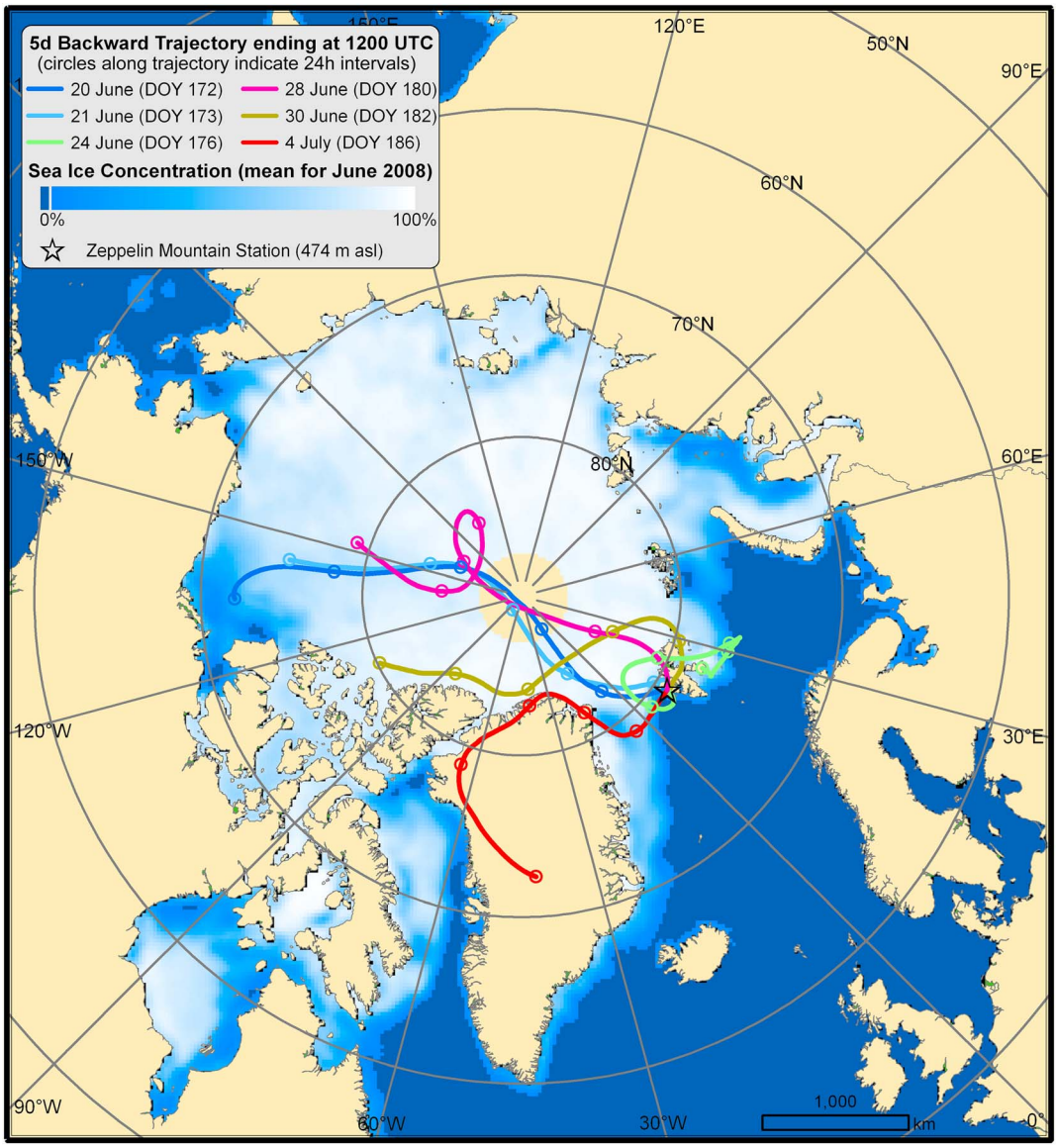

Figure 2. Air mass back-trajectories (5 days) arriving at the Zeppelin atmospheric research station (78.90°N, 11.88°E; 474 m asl) near Ny-Ålesund, Svalbard at 12:00 UTC on days when NPF events were observed. The trajectories were determined by the NOAA HYSPLIT model [*Draxler and Rolph*, 2015]. The sea ice concentration corresponds to the average June 2008 coverage [*NSIDC*, 2014].

chemical ionization mass spectrometer observed the presence of amine salts and that they were able to explain 23% of the growth of $D_p = 10$ nm particles [*Smith et al.*, 2010].

The presence of sulfuric acid was further investigated by analyzing whether its concentration ($[H_2SO_4]$) was correlated with the increase in N_{3-10} during NPF events. Although $[H_2SO_4]$ was not measured, a recent empirical proxy model [*Mikkonen et al.*, 2011] was used instead. The model is based on continental measurements and has not been previously tested for marine and Arctic conditions. However, as the model uses the SO_2 concentration regardless of whether it is derived from DMS or directly from SO_2, it is considered that the model can broadly estimate the H_2SO_4 concentration in the summertime Arctic.

The H_2SO_4 proxy concentration (molecules cm^{-3}) shown in Figure 3 was estimated using the following equation [*Mikkonen et al.*, 2011]:

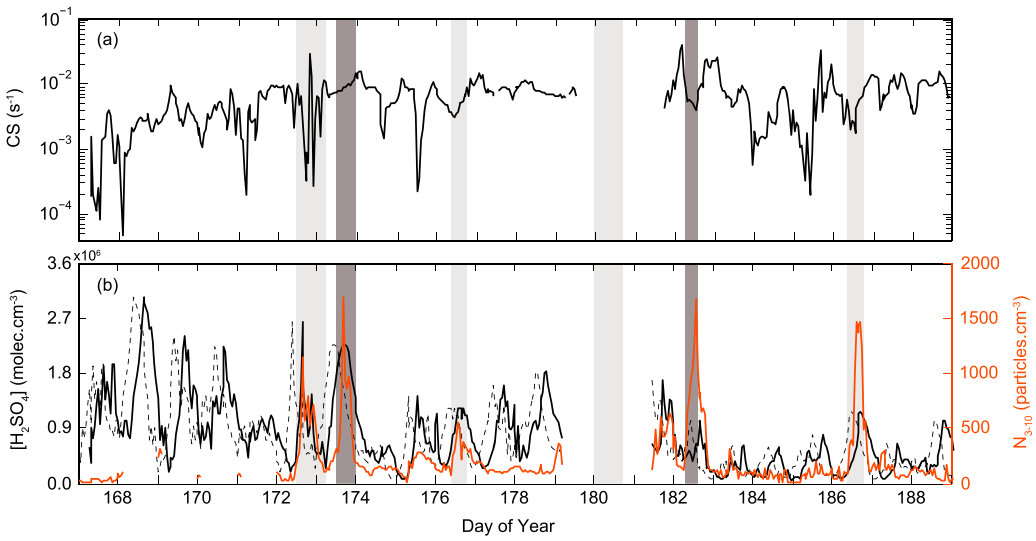

Figure 3. (a) Evolution of the hourly averaged condensation sink (CS) value. (b) The H_2SO_4 proxy concentration (black lines) and N_{3-10} concentration (red line) in the $D_p = 3$–10 nm range. Solid and dashed black lines correspond to hourly H_2SO_4 concentrations when shifted and not shifted by 6 h, respectively. Data for the H_2SO_4 proxy concentration calculations were provided by the Alfred Wegener Institute [*Maturilli et al.*, 2012].

$$[H_2SO_4] = 8.21\times10^{-3}\cdot k\cdot R\cdot [SO_2]^{0.62}\cdot (CS\cdot RH)^{-0.13} \quad (1)$$

where R is the global irradiation (W m^{-2}) and RH is the relative humidity (%). The parameters k (cm^3 molecules^{-1} s^{-1}) and CS (s^{-1}) [e.g., *Dal Maso et al.*, 2002] are a temperature-dependent reaction rate constant and the condensational sink, respectively, which are given by

$$k = \frac{A\cdot k_3}{(A+k_3)}\exp\left[k_5\left(1+\log_{10}\left(\frac{A}{k_3}\right)^2\right)^{-1}\right] \quad (2)$$

$$CS = 2\pi D\int_0^\infty d\beta_m(Dp)N(Dp)dDp = 2\pi D\sum\nolimits_i Dp_i\,\beta_i\,N_i \quad (3)$$

where $A = k_1[M](300/T)^{k_2}$, T(K) is the temperature, $[M] = 0.101\times(1.381\times10^{-23}\ T)^{-1}$ is the air density (molecules^{-1} cm^{-3}), $k_1 = 4\times10^{-31}$, $k_2 = 3.3$, $k_3 = 2\times10^{-12}$, and $k_5 = -0.8$. The predicted $[H_2SO_4]$ proxy values were between ~5.98×10^4 and 3.19×10^6 molecules cm^{-3} during the case study, which are similar to values measured in the Finnish sub-Arctic [*Mikkonen et al.*, 2011]. The model indicates that $[H_2SO_4]$ is driven by the variability in irradiation and relative humidity. In use of the model, we should point out that the predicted daily average values cannot be considered as absolute but rather as indicative of $[H_2SO_4]$ due to limitations of the empirical proxy model.

Regression analysis showed that the highest correlation ($R^2 \sim 0.7$) between the $[H_2SO_4]$ proxy and N_{3-10} occurs when a 6 h lag is applied to the calculated proxy (cf. Figure 3). This period can be attributed to the average time required for fresh clusters to grow above the CPC detection limit ($D_p > 3$ nm). In summary, the above aspects imply that sulfuric acid participated in nanoparticle formation and growth, which we explore further by providing observational evidence from volatility measurements.

Figure 4 illustrates VTDMA measurements of monodisperse particles ($D_p = 12$, 40, 200 nm) at thermodenuder temperatures $T_D = 30$, 120, 230°C. It should be noted that monodisperse particles either retained their sizes or shrank considerably, below the VTDMA detection limit (i.e., $D_p \sim 7$ nm), after passing through the thermodenuder. Particle volatility was therefore determined by comparing their number concentration before and after heat treatment. Figures 4a–4c show that nonevents were characterized by low particle number concentrations that consisted mainly of refractory components, in some cases

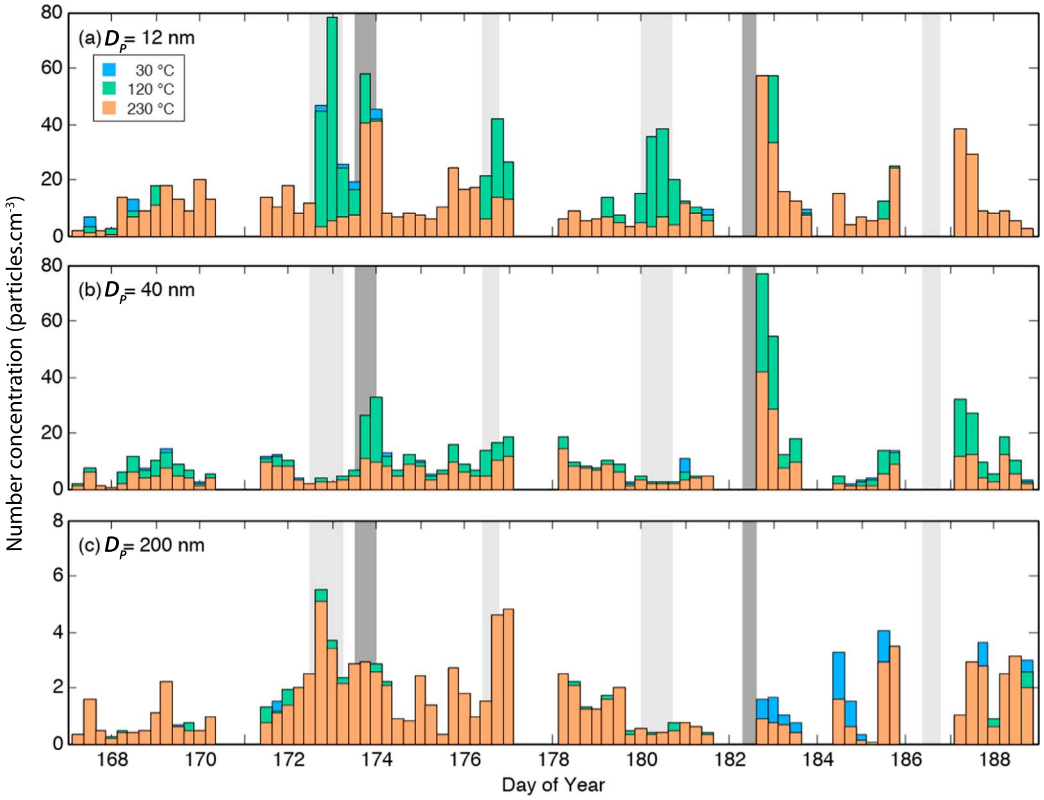

Figure 4. Monodisperse particle number concentrations measured by the VTDMA after thermodenuder processing. Stacked bars correspond to 30°C (blue), 120°C (green), and 230°C (orange) thermodenuder temperatures for (a) D_P = 12 nm particles, (b) 40 nm, and (c) 200 nm. Bar widths represent 6 h average values.

up to 100%. Although the composition of the refractory component using thermodenuder results cannot be determined here, previous volatility studies suggest that BC [*Nyeki et al.*, 2005] and sea-salt [*Clarke et al.*, 2006] may be involved but field observations at the sea ice interface [*Leck and Persson*, 1996; *Karl et al.*, 2013, and references therein], suggesting that their concentration and size distributions are unlikely to account for observations in this study. Recent studies [*Karl et al.*, 2013; *Leck et al.*, 2013; *Heintzenberg et al.*, 2015] point to the participation of nanogels and their building blocks in NPF, which raises the question as to whether they could also be components of the refractory fraction. This would have to be determined in a future case study. In contrast to these periods when a large fraction of the particle number concentration consisted of refractory particles, NPF events exhibited elevated particle number concentrations, especially for 12-nm particles. When the particles were treated in the thermodenuder, N_{12} decreased by 75—95% (average ~85%) at T_D = 230°C but remained unchanged at 120°C. This suggests that the majority of particles are solely composed of ammoniated sulfates with only a $\lesssim$15% number fraction composed of refractory components. Such behavior is in contrast to the observations during the anthropogenically influenced event on DOY 173 when N_{12} decreased by $<$20% at T_D = 230°C. The corresponding refractory number fraction of $>$80% is consistent with slightly enhanced BC concentrations during this event. Only one observation of a reduction (~10%) in N_{12} was made at T_D = 120°C on DOY 172, implying the presence of sulfuric acid particles.

For larger particles (Figures 4b and 4c), we observed that N_{40} decreased by $<$50%, N_{150} by $<$20% (not shown in Figure 3) and N_{200} by $<$15% at T_D = 230°C during NPF events. However, no changes in N_{40}, N_{150}, and N_{200} occurred at T_D = 120°C. This behavior again indicates the presence of ammoniated sulfates, with a clear decreasing trend in their number fraction as particle size increases. The corresponding increase in the number fraction of refractory particles with size suggests that the tail-end of the BC, sea salt [*Clarke et al.*, 2006], and/or nanogel [*Leck and Bigg*, 2005; *Karl et al.*, 2013] size distributions were being progressively observed. However, the refractory nature of nanogels remains to be demonstrated in a thermodenuder system.

As mentioned before, an alternative explanation of the particle volatility observations in terms of organic compounds rather than ammoniated sulfates is also possible. However, the fact that N_{12} does not decrease at thermodenuder temperatures up to 120°C, but drops by 75–95% at $T_D = 230$°C. is consistent with ammoniated sulfate particles. It should be mentioned that an unambiguous interpretation in terms of ammoniated sulfates cannot be made, as a single organic compound with similar volatility characteristics may have been present. For instance, *Qiu and Zhang* [2012] observed that alkylaminium sulfates with $D_p = 97$ nm have similar volatility characteristics to ammonium sulfate. Amine concentrations were not measured during our case-study, and as other measurements in the high Arctic are lacking, we are currently unable to assess their relative importance, if any.

Our volatility observations do not exclude the possibility that nanoparticles may have a nonvolatile core smaller than that measured by the VTDMA. If 12 nm particles were an internal mixture of ammoniated sulfates and a refractory component for instance, then an estimated shrinkage >80% by volume at $T_D = 230$°C would be required to reveal a nonvolatile core below our VTDMA detection limit at $D_p \sim 7$ nm. Clusters and nanoparticles that can serve as seeds for growth during NPF events are significantly smaller than this limit, making our measurements incapable of probing the early stages of NPF. However, a recent study [*Karl et al*., 2013] suggested that particles with $D_p < 7$ nm may consist of nanogel material. Simulation with an aerosol dynamics model revealed that the appearance of nanoparticles could only be explained by the presence of nonvolatile cores with a mean value of $D_p \sim 4.5$ nm.

4. Conclusions

In summary, the case-study measurements reported here support the hypothesis that the growth of 12 nm nanoparticles in the summertime high Arctic is driven by mechanisms involving sulfuric acid and ammonia. These particles can account for ~85% of the population during NPF events, four of which were studied here in detail and lasted from 10–13 h each. The remainder is attributed to refractory particles but can account for up to 100% of the population during nonevent days. Our observations further suggest that the majority of the sub-40 nm particle population during NPF events does not exist in the form of sulfuric acid but rather as partly or fully neutralized ammoniated sulfates. Considering the observed spatial and temporal extent of NPF events in the summertime high Arctic [*Kulmala et al*., 2004; *Karl et al*., 2012; *Leaitch et al*., 2013; *Tunved et al*., 2013], our observations on Svalbard suggest that ammoniated sulfate nanoparticles may be more ubiquitous in this region than previously thought. However, several important aspects would need to be addressed in greater detail. One concerns a more detailed understanding of NPF events with respect to both the pack-ice region, and the impact of local mixing and long-range advection/transport. Another aspect concerns the sources and abundance of precursor gases (e.g., NH_3 and amines) in the high Arctic. A more comprehensive study with simultaneous measurements over the pack-ice region and on Svalbard in the future would help to resolve some of these aspects.

Acknowledgments
The fieldwork data in this study have been acquired in collaboration with J. Ondracek and A. Karanasiou and funded by ARCFAC: Transnational access to the Ny-Ålesund Research Infrastructure, EC/FP6 program grant ARCFAC-026129-2008-14. Data analysis was jointly funded by EnTeC FP7 Capacities program (REGPOT-2012-2013-1, FP7, ID:316173), the European Social Fund, and the Greek National Strategic Reference Framework program Heracleitus II. Thanks are due to E. Papapanagiotou for producing the trajectory map shown in the supporting information. The data generated in this study are available from the authors upon request (elefther@ipta.demokritos.gr).

References

Aas, W., S. Solberg, S. Manø, and K. E. Yttri (2012), Monitoring of long-range transported air pollutants. Annual report 2011, Tech. Rep. Norwegian Klif report 126/2012. NILU OR 19/2012, Norwegian Inst. for Air Res., Kjeller, Norway.

Almeida, J., et al. (2013), Molecular understanding of sulphuric acid–amine particle nucleation in the atmosphere, *Nature*, *502*, 359–363, doi:10.1038/nature12663.

Bigg, E. K., and C. Leck (2001), Properties of the aerosol over the central Arctic Ocean, *J. Geophys. Res.*, *106*(D23), 32,101–32,109.

Chang, R. Y.-W., S. J. Sjostedt, J. R. Pierce, T. N. Papakyriakou, M. G. Scarratt, S. Michaud, M. Levasseur, W. R. Leaitch, and J. P. D. Abbatt (2011), Relating atmospheric and oceanic DMS levels to particle nucleation events in the Canadian Arctic, *J. Geophys. Res.*, *116*, D00S03, doi:10.1029/2011JD015926.

Chen, M., et al. (2012), Acid–base chemical reaction model for nucleation rates in the polluted atmospheric boundary layer, *Proc. Natl. Acad. Sci. U.S.A.*, *109*, 18,713–18,718, doi:10.1073/pnas.1210285109.

Clarke, A. (1991), A thermo-optic technique for in situ analysis of size-resolved aerosol physicochemistry, *Atmos. Environ.*, *25A*, 635–644.

Clarke, A. D., S. R. Owens, and J. C. Zhou (2006), An ultrafine sea-salt flux from breaking waves: Implications for cloud condensation nuclei in the remote marine atmosphere, *J. Geophys. Res.*, *111*, D06202, doi:10.1029/2005JD006565.

Covert, D., and J. Heintzenberg (1993), Size distributions and chemical-properties of aerosol at Ny Alesund, Svalbard, *Atmos. Environ.*, *27*, 2989–2997, doi:10.1016/0960-1686(93)90331-R.

Dal Maso, M., M. Kulmala, K. E. J. Lehtinen, J. M. Mäkelä, P. Aalto, and C. D. O'Dowd (2002), Condensation and coagulation sinks and formation of nucleation mode particles in coastal and boreal forest boundary layers, *J. Geophys. Res.*, *107*(D19), 8097, doi:10.1029/2001JD001053.

Draxler, R. R., and G. D. Hess (1997), Description of the HYSPLIT 4 modeling system, NOAA Tech. Memo. ERL ARL-224, 24 pp., NOAA Air Resources Lab., Silver Spring, Md.

Draxler, R. R., and G. D. Rolph (2015), *HYSPLIT (HYbrid Single-Particle Lagrangian Integrated Trajectory) Model*, NOAA Air Resources Lab., Silver Spring, Md. [Available at http://ready.arl.noaa.gov/HYSPLIT.php.]

Ehn, M., et al. (2014), A large source of low-volatility secondary organic aerosol, *Nature*, *505*, 476–479, doi:10.1038/nature13032.
Eleftheriadis, K., S. Nyeki, C. Psomiadou, and I. Colbeck (2004), Background aerosol properties in the European Arctic, *Water, Air Soil Pollut. Focus*, *4*, 23–30, doi:10.1023/B:WAFO.0000044783.70114.19.
Eleftheriadis, K., S. Vratolis, and S. Nyeki (2009), Aerosol black carbon in the European Arctic: Measurements at Zeppelin Station, Ny-Alesund, Svalbard from 1998–2007, *Geophys. Res. Lett.*, *36*, L02809, doi:10.1029/2008GL035741.
EMEP, (2014) Manual for sampling and chemical analysis. Kjeller, Norwegian Inst. for Air Res. (EMEP/CCC Report 1/95) (Last rev. February 2014). [Available at http://www.nilu.no/projects/ccc/manual/index.html.]
Engvall, A.-C., R. Krejci, J. Strom, R. Treffeisen, R. Scheele, O. Hermansen, and J. Paatero (2008), Changes in aerosol properties during spring-summer period in the Arctic troposphere, *Atmos. Chem. Phys.*, *8*, 445–462. [Available at www.atmos-chem-phys.net/8/445/2008/.]
Fierz, M., M. G. C. Vernooij, and H. Burtscher (2007), An improved low-flow thermodenuder, *J. Aerosol Sci.*, *38*, 1163–1168, doi:10.1016/j.jaerosci.2007.08.006.
Frey, A., D. Rose, B. Wehner, T. Mueller, Y. Cheng, A. Wiedensohler, and A. Virkkula (2008), Application of the volatility-TDMA technique to determine the number size distribution and mass concentration of less volatile particles, *Aerosol Sci. Technol.*, *42*, 817–828, doi:10.1080/02786820802339595.
Ge, X., A. S. Wexler, and S. L. Clegg (2010), Atmospheric amines – Part I., A review, *Atmos. Environ.*, *45*, 524–546.
Geng, H., J.-Y. Ryu, H.-J. Jung, H. Chung, K.-H. Ahn, and C.-U. Ro (2010), Single-particle characterization of summertime Arctic aerosols collected at Ny-Alesund, Svalbard, *Environ. Sci. Technol.*, *44*, 2348–2353, doi:10.1021/es903268j.
Hakkinen, S. A. K., et al. (2012), Long-term volatility measurements of submicron atmospheric aerosol in Hyytiälä, Finland, *Atmos. Chem. Phys.*, *12*, 10,771–10,786, doi:10.5194/acp-12-10771-2012.
Heintzenberg, J., and C. Leck (1994), Seasonal-variation of the atmospheric aerosol near the top of the marine boundary-layer over Spitsbergen related to the Arctic sulfur cycle, *Tellus Ser. B-Chem. Phys. Meteorol.*, *46*, 52–67, doi:10.1034/j.1600-0889.1994.00005.x.
Heintzenberg, J., C. Leck, and P. Tunved (2015), Potential source regions and processes of aerosol in the summer Arctic, *Atmos. Chem. Phys.*, *15*, 6487–6502, doi:10.5194/acp-15-6487-2015.
Karl, M., C. Leck, A. Gross, and L. Pirjola (2012), A study of new particle formation in the marine boundary layer over the central Arctic ocean using a flexible multicomponent aerosol dynamic model, *Tellus Ser. B-Chem. Phys. Meteorol.*, *64*, 17,158, doi:10.3402/tellusb.v64i0.17158.
Karl, M., C. Leck, E. Coz, and J. Heintzenberg (2013), Marine nanogels as a source of atmospheric nanoparticles in the high Arctic, *Geophys. Res. Lett.*, *40*, 3738–3743, doi:10.1002/grl50661.
Keady, P. B., F. R. Quant, and G. J. Sem (1983), Differential mobility particle sizer: A new instrument for high-resolution aerosol size distribution measurement below 1 μm, *TSI Quart.*, *9*(2), 3–11.
Korhonen, P., M. Kulmala, A. Laaksonen, Y. Viisanen, R. McGraw, and J. H. Seinfeld (1999), Ternary nucleation of H_2SO_4, NH_3, and H_2O in the atmosphere, *J. Geophys. Res.*, *104*, 26,349–26,353, doi:10.1029/1999JD900784.
Kuang, C., I. Riipinen, S.-L. Sihto, M. Kulmala, A. V. McCormick, and P. H. McMurry (2010), An improved criterion for new particle formation in diverse atmospheric environments, *Atmos. Chem. Phys.*, *10*, 8469–8480, doi:10.5194/acp-10-8469-2010.
Kulmala, M., H. Vehkamaki, T. Petaja, M. Dal Maso, A. Lauri, V. M. Kerminen, W. Birmili, and P. H. McMurry (2004), Formation and growth rates of ultrafine atmospheric particles: A review of observations, *J. Aerosol Sci.*, *35*, 143–176, doi:10.1016/j.jaerosci.2003.10.003.
Kulmala, M., et al. (2013), Direct observations of atmospheric aerosol nucleation, *Science*, *339*, 943–46, doi:10.1126/science.1227385.
Leaitch, W. R., et al. (2013), Dimethyl sulfide control of the clean summertime Arctic aerosol and cloud, *Elementa: Sci. Anthropocene*, *1*, 000017, doi:10.12952/journal.elementa.000017.
Leck, C., and E. K. Bigg (1999), Aerosol production over remote marine areas - A new route, *Geophys. Res. Lett.*, *26*, 3577–3580, doi:10.1029/1999GL010807.
Leck, C., and E. K. Bigg (2005), Biogenic particles in the surface microlayer and overlaying atmosphere in the central Arctic Ocean during summer, *Tellus B*, *57*, 305–316, doi:10.1111/j.1600-0889.2005.00148.x.
Leck, C., and E. K. Bigg (2010), New particle formation of marine biological origin, *Aerosol Sci. Technol.*, *44*, 570–577, doi:10.1080/02786826.1010.481222.
Leck, C., and C. Persson (1996), Seasonal and short-term variability in dimethyl sulfide, sulfur dioxide and biogenic sulfur and sea salt aerosol particles in the arctic marine boundary layer, during summer and autumn, *Tellus B*, *48*, 272–299.
Leck, C., Q. Gao, F. Mashayekhy Rad, and U. Nilsson (2013), Size-resolved atmospheric particulate polysaccharides in the high summer Arctic, *Atmos. Chem. Phys.*, *13*, 12,573–12,588, doi:10.5194/acp-13-12573-2013.
Maturilli, M., et al. (2012), *Continuous Meteorological Observations at Station Ny-Ålesund (2008–07)*, Alfred Wegener Institute for Polar and Marine Research - Research Unit, Potsdam, doi:10.1594/PANGAEA.775676, In Supplement to: Maturilli, Marion; Herber, Andreas; Kφnig-Langlo, Gert (2013): Climatology and Time Series of Surface Meteorology in Ny-Ålesund, Svalbard. Earth System Science Data, 5(1), 155–163, doi:10.5194/essd-5-155-2013.
McMurry, P. H. (2000), A review of atmospheric aerosol measurements, *Atmos. Environ.*, *34*, 1959–1999, doi:10.1016/S1352-2310(99)00455-0.
Mendes, L., K. Eleftheriadis, and G. Biskos (2016), Performance comparison of two thermodenuders in volatility tandem DMA measurements, *J. Aerosol Sci.*, *92*, 38–52, doi:10.1016/j.jaerosci.2015.10.002.
Mikkonen, S., et al. (2011), A statistical proxy for sulphuric acid concentration, *Atmos. Chem. Phys.*, *11*, 11,319–11,334, doi:10.5194/acp-11-11319-2011.
NSIDC (2014), National Snow and Ice Data Center. [Available at http://nsidc.org/(9/2/2014).]
Nyeki, S., G. Coulson, I. Colbeck, K. Eleftheriadis, U. Baltensperger, and H. J. Beine (2005), Overview of aerosol microphysics at Arctic Sunrise: Measurements during the NICE renoxification study, *Tellus Ser. B-Chem. Phys. Meteorol.*, *57*, 40–50, doi:10.1111/j.1600-0889.2005.00122.x.
O'Dowd, C. D., J. L. Jimenez, R. Bahreini, R. C. Flagan, J. H. Seinfeld, K. Hameri, L. Pirjola, M. Kulmala, S. G. Jennings, and T. Hoffmann (2002), Marine aerosol formation from biogenic iodine emissions, *Nature*, *417*, 632–636, doi:10.1038/nature00775.
Paasonen, P., et al. (2012), On the formation of sulphuric acid - amine clusters in varying atmospheric conditions and its influence on atmospheric new particle formation, *Atmos. Chem. Phys.*, *12*, 9113–9133, doi:10.5194/acp-12-9113-2012.
Qiu, C., and R. Zhang (2012), Physiochemical properties of alkylaminium sulfates: Hygroscopicity, thermostability, and density, *Environ. Sci. Technol.*, *46*, 4474–4480, doi:10.1021/es3004377.
Riccobono, F., et al. (2014), Oxidation products of biogenic emissions contribute to nucleation of atmospheric particles, *Science*, *344*, 717–721, doi:10.1126/science.1243527.
Riipinen, I., T. Yli-Juuti, J. R. Pierce, T. Petaja, D. R. Worsnop, M. Kulmala, and N. M. Donahue (2012), The contribution of organics to atmospheric nanoparticle growth, *Nat. Geosci.*, *5*, 453–458, doi:10.1038/ngeo1499.
Sakurai, H., M. A. Fink, P. H. McMurry, L. Mauldin, K. F. Moore, J. N. Smith, and F. L. Eisele (2005), Hygroscopicity and volatility of 4–10 nm particles during summertime atmospheric nucleation events in urban Atlanta, *J. Geophys. Res.*, *110*, D22S04, doi:10.1029/2005JD005918.

Sipila, M., et al. (2010), The role of sulfuric acid in atmospheric nucleation, *Science*, *327*, 1243–1246, doi:10.1126/science.1180315.
Smith, J. M., K. C. Barsanti, H. R. Friedli, M. Ehn, M. Kulmala, D. R. Collins, J. H. Scheckman, B. J. Williams, and P. H. McMurry (2010), Observations of aminium salts in atmospheric nanoparticles and possible climatic implications, *Proc. Natl. Acad. Sci. U.S.A.*, *107*, 6634–6639, doi:10.1073/pnas.0912127107.
Stolzenburg, M. R., and P. H. McMurry (1991), An ultrafine aerosol condensation nucleus counter, *Aerosol Sci. Technol.*, *14*, 48–65.
Tørseth, K., W. Aas, K. Breivik, A. M. Fjæraa, M. Fiebig, A. G. Hjellbrekke, C. Lund Myhre, S. Solberg, and K. E. Yttri (2012), Introduction to the European Monitoring and Evaluation Programme (EMEP) and observed atmospheric composition change during 1972–2009, *Atmos. Chem. Phys.*, *12*, 5447–5481, doi:10.5194/acp-12-5447-2012.
Tunved, P., H. C. Hansson, V. M. Kerminen, J. Strom, M. Dal Maso, H. Lihavainen, Y. Viisanen, P. P. Aalto, M. Komppula, and M. Kulmala (2006), High natural aerosol loading over boreal forests, *Science*, *312*, 261–263, doi:10.1126/science.1123052.
Tunved, P., J. Strom, and R. Krejci (2013), Arctic aerosol life cycle: Linking aerosol size distributions observed between 2000 and 2010 with air mass transport and precipitation at Zeppelin Station, Ny-Alesund, Svalbard, *Atmos. Chem. Phys.*, *13*, 3643–3660, doi:10.5194/acp-13-3643-2013.
Villani, P., D. Picard, N. Marchand, and P. Laj (2007), Design and validation of a 6-volatility tandem differential mobility analyzer (VTDMA), *Aerosol Sci. Technol.*, *41*, 898–906, doi:10.1080/02786820701534593.
Wang, L., V. Lal, A. F. Khalizov, and R. Zhang (2010), Heterogeneous chemistry of alkylamines with sulfuric acid: Implications for atmospheric formation of alkylaminium sulfates, *Environ. Sci. Technol.*, *44*, 2461.
Weber, R. J., J. J. Marti, P. H. McMurry, F. L. Eisele, D. J. Tanner, and A. Jefferson (1996), Measured atmospheric new particle formation rates: Implications for nucleation mechanisms, *Chem. Eng. Commun.*, *151*, 53–64, doi:10.1080/00986449608936541.
Wiedensohler, A., D. S. Covert, E. Swietlicki, P. Aalto, J. Heintzenberg, and C. Leck (1996), Occurrence of an ultrafine particle mode less than 20 nm in diameter in the marine boundary layer during Arctic summer and autumn, *Tellus Ser. B-Chem. Phys. Meteorol.*, *48*, 213–222, doi:10.1034/j.1600-0889.1996.t01-1-00006.x.
Yli-Juuti, T., et al. (2011), Growth rates of nucleation mode particles in Hyytiälä during 2003–2009: Variation with particle size, season, data analysis method and ambient conditions, *Atmos. Chem. Phys.*, *11*, 12,865–12,886, doi:10.5194/acp-11-12865-2011.
Yli-Juuti, T., K. Barsanti, L. Hildebrandt Ruiz, A.-J. Kieloaho, U. Makkonen, T. Petaja, T. Ruuskanen, M. Kulmala, and I. Riipinen (2013), Model for acid–base chemistry in nanoparticle growth (MABNAG), *Atmos. Chem. Phys.*, *13*, 12,507–12,524, doi:10.5194/acp-13-12507-2013.
Zhang, R., A. Khalizov, L. Wang, M. Hu, and W. Xu (2012), Nucleation and growth of nanoparticles in the atmosphere, *Chem. Rev.*, *112*, 1957–2011, doi:10.1021/cr2001756.